Electrogenerated Chemiluminescence. 74. Photophysical, Electrochemical, and Electrogenerated Chemiluminescent Studies of Selected Nonplanar Pyrenophanes

Rebecca Y. Lai,[†] James J. Fleming,[†] Brad L. Merner,[†] Rudolf J. Vermeij,[†] Graham J. Bodwell,[‡] and Allen J. Bard*,[†]

Department of Chemistry and Biochemistry, The University of Texas at Austin, Austin, Texas 78712, and Department of Chemistry, Memorial University of Newfoundland, St. John's, NL, Canada A1B 3X7

Received: September 18, 2003; In Final Form: November 4, 2003

We report here the photophysical, electrochemical, and electrogenerated chemiluminescent studies of four new pyrenophanes. Comparison with the cyclic voltammogram obtained using the planar parent compound, pyrene, showed these bent-pyrene-containing cyclophanes have a shift in the thermodynamic reduction potentials to more negative values. AM1 semiempirical calculations support such findings in which the LUMO energy increased with the degree of nonplanarity. The HOMO energy, however, remained essentially unchanged for all the compounds in this study. The nonplanarity in these compounds resulted in a substantial decrease in fluorescence quantum yield as well as a slight red shift in both the absorption and emission spectra. In addition, unlike pyrene, no excimer emission was evident in the fluorescence spectra even at concentrations as high as 1 mM. However, the ECL spectra of all four pyrenophanes, produced by generating the anion radical in the presence of benzoyl peroxide as a coreactant, showed broad "excimer-like" emission in addition to the monomer emission observed at shorter wavelengths.

Introduction

Many PAHs have been employed in the study of electrogenerated chemiluminescence (ECL), in both fundamental and applicational-oriented research.[1] Pyrene has been the subject of a number of ECL studies, which have demonstrated the formation of the excited singlet state by annihilation of the radical ions in addition to the presence of extensive excimer emission.[2,3] Bodwell and co-workers have recently synthesized and studied pyrenophanes containing nonplanar pyrene moieties and we thought it would be of interest to see the extent to which nonplanarity of the pyrene affects the electrochemical and ECL response.[4,5] We show in this paper photophysical and electrochemical characterization of several nonplanar pyrenophanes (Figure 1a), as well as the ECL that results from both the radical ion annihilation and the use of a coreactant, benzoyl peroxide (BPO). Classical ECL involves electron transfer between electrochemically generated species, often radical ions, which results in an excited species that emits light. The simplest ECL process is the radical ion annihilation reaction, which can be represented as

$$D + e^- \rightarrow D^{\bullet -} \quad \text{(reduction at electrode)} \tag{1}$$

$$D - e^- \rightarrow D^{\bullet +} \quad \text{(oxidation at electrode)} \tag{2}$$

$$D^{\bullet -} + D^{\bullet +} \rightarrow {}^1D^* + D \quad \text{(singlet excited state formation)} \tag{3}$$

$$D^{\bullet -} + D^{\bullet +} \rightarrow {}^3D^* + D \quad \text{(triplet excited state formation)} \tag{4}$$

$${}^3D^* + {}^3D^* \rightarrow {}^1D^* + D \quad \text{(triplet−triplet annihilation)} \tag{5}$$

$${}^1D^* \rightarrow D + h\nu_1 \quad \text{(monomer light emission)} \tag{6}$$

where D, for example, is a polycyclic aromatic hydrocarbon (PAH).[1] The ECL spectrum usually resembles the fluorescence spectrum of the compound in the same solvent. However, ECL spectra of PAHs such as pyrene and perylene also show broad emission peaks at longer wavelengths than the normal emission. They have been attributed to the emission of excimers or to decomposition products generated upon during the annihilation reactions.[2,6,7] Such ECL processes can be represented as

$$D^{\bullet -} + D^{\bullet -} \rightarrow {}^1D_2^* \quad \text{(annihilation/excimer formation)} \tag{7}$$

$${}^1D^* + D \rightarrow {}^1D_2^* \quad \text{(excimer formation)} \tag{8}$$

$${}^1D_2^* \rightarrow 2D + h\nu_2 \quad \text{(excimer light emission)} \tag{9}$$

In some situations, however, the radical cation or anion cannot be generated prior to the background oxidation or reduction of the solvent/supporting electrolyte used for electrochemistry. In this case, a second compound must be added to generate a stable radical counterion (a second reductant or oxidant to react with the radical cation or anion) required for annihilation. In recent years, an important advance in ECL was the discovery of reaction schemes for generating ECL via the use of coreactants or other electrogenerated species capable of reacting with either

* To whom correspondence should be addressed: ajbard@mail.utexas.edu.
[†] The University of Texas at Austin.
[‡] Memorial University of Newfoundland.

10.1021/jp0367981 CCC: $27.50
Published on Web 12/23/2003

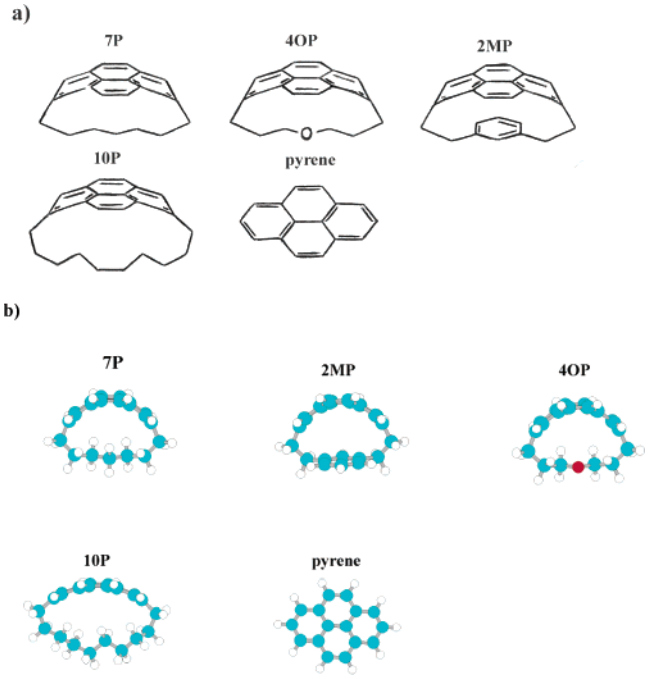

Figure 1. (a) Molecular structures of pyrene and pyrenophanes. (b) Optimized ground-state molecular geometry of the same compounds as calculated by AM1 semiempirical calculations.

the anion or cation alone to produce the desired excited state. These reactions could be observed on the basis of their ability to generate energetic precursors at less extreme potentials upon bond cleavage of a coreactant such as oxalate, peroxydisulfate, and BPO.[8−10]

We report here a new class of nonplanar pyrene derivatives capable of ECL. The five compounds studied were chosen on the basis of their chemical structures, as are shown in Figure 1a. The selected pyrenophanes were [10](2,7)pyrenophane (10P), [7](2,7)pyrenophane (7P), [2]metacyclo[2](2,7)pyrenophane (2MP), and 4-oxa[7](2,7)pyrenophane (4OP).The fluorescence and electrochemical properties of these compounds were investigated to locate energies and evaluate their potential for ECL. The results obtained from these four pyrenophanes are compared with the parent compound, pyrene, in an attempt to understand how deviation from planarity might affect their electrochemical, photophysical, and ECL behavior. These results provide further insight into future development of similar compounds for ECL.

Experimental Section

2MP, 7P, 4OP, and 10P provided by Bodwell et al. were synthesized as described elsewhere.[4,5] The supporting electrolyte, tetra-*n*-butylammonium hexafluorphosphate ($TBAPF_6$), was recrystallized twice and dried in a vacuum oven at 100 °C prior to transferring it directly into an inert atmosphere drybox (Vacuum Atmospheres Corp., Hawthorne, CA). Pyrene (Aldrich, St. Louis, MO), anhydrous benzene (PhH) (Aldrich, ACS spectrophotometric grade) and anhydrous acetonitrile (MeCN) (Aldrich, ACS spectrophotometric grade) were used without further purification. All solutions were prepared in the drybox with fresh anhydrous solvents and sealed in airtight vessels for measurements completed outside the drybox. All fluorescence spectra were recorded on a QuantaMaster Model QM-1 spectrofluorimeter (Photon Technology International, Lawrenceville, NJ) modified with a continuous wave excitation lightsource. In all cases, a slit width of 2 nm and a resolution of 1 nm were used. All UV−visible spectra were recorded on a Milton Roy Spectronic 3000 array spectrophotometer. The absorbance and fluorescence spectrum of the four pyrenophanes were obtained with a 20 μM solution prepared with MeCN. The relative fluorescence efficiency was measured using a 20 μM solution in MeCN compared to pyrene as a standard. (λ_{exc} =334 nm; Φ_{pyrene} = 0.60 in PhH).[11]

Cyclic voltammograms were recorded on a CH Instruments Electrochemical Work Station (Austin, TX). A platinum disk electrode (1.5 or 2 mm in diameter) was used as the working electrode, and a platinum wire was used as the auxiliary electrode. A silver wire was used as a quasi-reference electrode. The potentials were calibrated versus SCE by the addition of ferrocene as an internal standard using $E°(Fc/Fc^+)$ = 0.424 V vs SCE.[12] All solutions were prepared in the drybox with fresh anhydrous solvents and sealed in airtight vessels for measurements completed outside the drybox. The concentration used to obtain each voltammogram or ECL spectrum is given in the corresponding figure caption.

All ECL measurements were performed as previously reported.[13] To generate ECL via radical ion annihilation, the working electrode was pulsed between the oxidation and reduction peak potentials of each compound with a pulse width of 0.1 s. The resulting emission spectra were obtained with a charged coupled device (CCD) camera that was cooled to −100 °C. Integration times were 2 min. In the presence of a coreactant, the working electrode was pulsed between 0 V and the reduction peak potential of the compound of interest.

Results and Discussion

Absorption and Emission Spectroscopy. Absorption and fluorescence spectra of pyrene and the four pyrenophanes are shown in Figure 2a,b. The absorption spectra were obtained in the same solvent mixture used for all electrochemical measurements, with the exceptions of pyrene and 10P. As observed, the absorption spectra of all five compounds showed three sets of absorption bands, the β', β, and p bands, ranging from 220 to 350 nm. For 2MP, 4OP, and 7P, the more distorted pyrenophanes, the overlapping β' and β bands were broad and featureless, ranging from 250 to 300 nm. These bands are shifted to lower energy by about 20 nm when compared to 10P, the least strained pyrenophane in this study. The absorption spectrum of 10P showed resemblances to the spectrum of pyrene in terms of band shape and was characterized by highly resolved β' and β bands, each with two defined vibrational modes. However, the wavelengths of the β' and β bands are still slightly red-shifted when compared to pyrene, probably due to the substitutions at the 2 and 7 positions. We were, however, more interested in the p bands, which could be used to determine the lowest singlet energy of these compounds. Previous research has also shown that the p bands should not shift significantly until the distortion becomes pronounced and a slight blue shift would be observed.[14] Among the four pyrenophanes, 10P showed the lowest energy p absorption bands (340 nm) whereas 2MP displayed the highest energy p bands (337 nm), suggesting that 2MP is the most distorted pyrenophane in this series of compounds. Additionally, the intensities of the p bands of 2MP, 4OP, and 7P are much weaker than those of 10P and pyrene, which agree well with previous studies from Bodwell et al.[14] A summary of the spectroscopic data is given in Table 1.

The fluorescence spectra of the five compounds are shown in Figure 2b. 2MP and 4OP exhibited broad, structureless blue fluorescence centered around 423 and 429 nm, respectively. 7P showed two smaller vibrational structures around 380 and 390

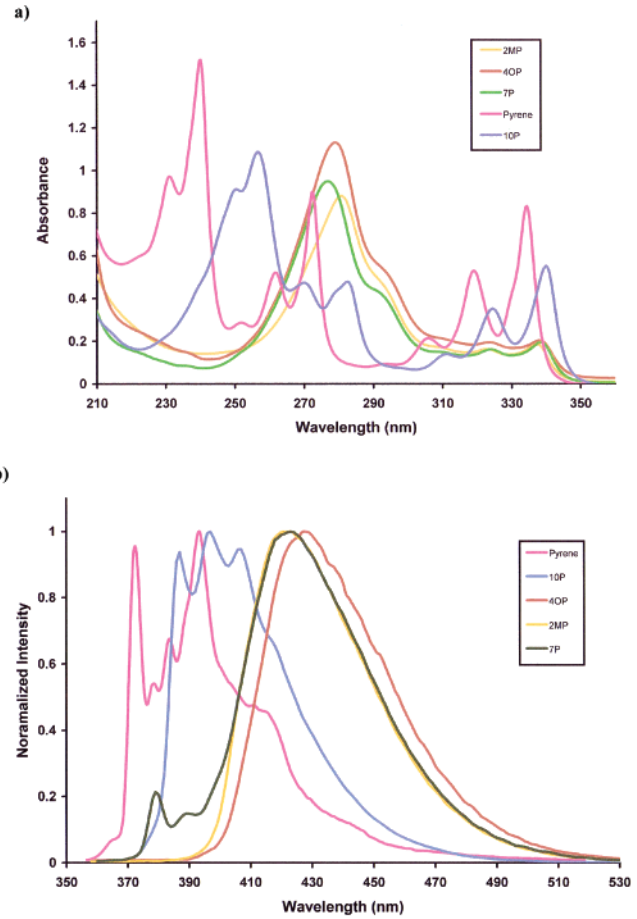

Figure 2. (a) Optical absorption and (b) normalized fluorescence spectra of 20 μM of 2MP (yellow), 4OP (orange), 7P (green), pyrene (magenta), and 10P (blue) in MeCN. Excitation wavelength: 338 nm for 2MP, 339 nm for 4OP, 340 nm for 7P, 335 nm for pyrene, and 342 nm for 10P.

nm in addition to a broad emission band with observed maxima of 424 nm. The emission spectrum of 10P is slightly blue-shifted (20 nm) from the rest of the pyrenophanes, characterized by three defined vibrational structures around 387, 397, and 407 nm, similar to the vibrational structures observed in a typical fluorescence spectrum of pyrene. A relatively large Stokes shift of 80 nm was observed between the absorption and emission maxima of 2MP and 4OP whereas a smaller Stokes shift, 47 nm, was observed in 10P, the least strained pyrenophane in this study. However, the Stokes shift observed in 10P was still greater than in pyrene, which showed a shift of 38 nm. An increase in Stokes shift is observed with increasing degree of bending, probably owing to the changes in the molecular structure of the compound upon excitation. In particular, the difference in energy between the geometrically relaxed ground state and the nonrelaxed excited singlet state is larger than the energy difference between the geometrically relaxed excited state and the nonrelaxed ground state.[15] In addition, an increase in Stokes shift in larger and more flexible compounds could also be due to solvent rearrangement in the transient ground state and singlet-excited state.

Compared to pyrene as a standard, the fluorescence efficiencies of 10P, 2MP, 7P, and 4OP measured in MeCN are 0.54, 0.38, 0.37, and 0.19, respectively.[11] Overall, the observed fluorescence efficiencies appear to decrease with increasing nonplanarity, with 10P being the most efficient. The differences in fluorescence efficiency among the pyrenophanes are probably due to differences in the rate of nonradiative deactivation such as internal conversion, which is directly related to the lack of planarity in a molecule. The unusually low quantum efficiency observed for 4OP could also be attributed to the presence of the oxygen atom in the aliphatic bridge across the 2 and 7 positions. Pyrene, a planar PAH, is also known to exhibit excimer emission at concentrations above 300 μM.[16] However, no excimer emission was observed from any of the pyrenophanes in this study, even at concentrations up to 1 mM. On the basis of the optimized ground state geometry from AM1 calculations for these four pyrenophanes (Figure 1b), the severe distortion in these compounds probably minimizes intermolecular interaction and, therefore, impedes excimer formation within the lifetime of the molecular excited state.[17]

In summary, based on the emission wavelengths in the fluorescence spectra (Figure 2b), the energy needed to generate the first singlet-excited state of each of these compounds ranges from 2.9 to 3.2 eV. This energy must be generated in the electrochemical annihilation reaction of the radical ions or in the presence of a coreactant to generate directly the singlet excited state and ECL emission. Detailed summary of the spectroscopic data as well as ECL results are tabulated in Table 1.

Electrochemistry. Cyclic voltammetry was used to investigate the effects of various aliphatic bridges across positions 2 and 7 on the pyrene ring system, with the aim of finding correlations between the standard redox potentials (E_p or $E_{1/2}$), and the degree of bending in the molecule, as found in previous studies.[4,14] Electrochemical results are summarized in Table 2. Cyclic voltammograms (CV) of the four pyrenophanes and pyrene in 0.1 M $TBAPF_6$ in MeCN or MeCN/PhH obtained at a platinum electrode are shown in Figure 3. As observed, all of the compounds, except 10P, displayed an irreversible oxidation and a reversible reduction in MeCN or MeCN/PhH.

In MeCN, 2MP, the pyrenophane with a single *m*-phenylene unit in the aliphatic bridge, showed a one-electron irreversible oxidation wave at peak potential of 1.18 V vs SCE. Reversibility was not obtained for the oxidation wave even at scan rates beyond 50 V/s. The irreversibility in the oxidation of the radical cation is probably due to a following chemical reaction with trace water or the solvent, acetonitrile. The chemical byproducts generated were reducible at different potentials on scan reversal by the reduction waves around 0.27 and 0 V vs SCE, as observed in Figure 3a. Upon scanning in the negative direction, a reversible one-electron reduction wave was obtained at a half-wave potential of -2.41 V vs SCE. The observed peak separation for this reversible reduction wave was about 100 mV, larger than that expected for nernstian behavior where a one-electron wave is expected to have a peak separation of 59 mV. However, the internal standard, ferrocene, which is known to show nernstian behavior, showed a similar peak separation under the same conditions; thus, the observed peak separation can be attributed to ohmic drop ($\sim$1 kΩ) that is often observed within aprotic solvents. Additionally, the peak current ratio (i_{pc}/i_{pa}) was approximately unity down to a scan rate of 100 mV/s, indicating that the reduction to the radical anion is near stable. However, upon reversing potential, two new small oxidation waves appeared at -1.3 and -0.04 V vs SCE (Figure 3a). These waves probably correspond to the oxidations of the protonated compounds or other chemical byproducts that are easier to oxidize than the parent compound.

4OP showed similar electrochemical behavior as to 2MP; however, the reduction peak current ratio (i_{pc}/i_{pa}) was approximately unity only down to a scan rate of 500 mV/s, suggesting the presence of following chemical reactions that

TABLE 1: Spectroscopic and ECL Data for Various Compounds

compound (solvent)	$\lambda_{max(Abs)}$ (*p* band) (nm)	$\lambda_{max(PL)}$ (nm)	E_{S1-S0} (eV)	$\Phi_{(PL)}$	$\lambda_{max(ECL)}$ (via annihilation) (nm)	$\lambda_{max(ECL)}$ (with BPO) (nm)
2MP (MeCN)	337.3	422	2.94	0.38		430, 590
7P (MeCN)	338.5	423	2.93	0.37		439, 603
4OP (MeCN)	338.5	429	2.89	0.19		444, 607
10P (MeCN/PhH)	340.7	397	3.13 (MeCN)	0.54	414, 587, 681	420, 589
pyrene (MeCN/PhH)	334.5	393	3.16 (MeCN)	0.60	513, 644	418, 514

TABLE 2: Comparison between HOMO and LUMO Energies and Voltammetric and Spectroscopic Data

compound (solvent)	$E_{p(R/R+)}$ (V vs SCE)	$E_{1/2(R/R-)}$ (V vs SCE)	$\Delta E_{p-1/2}$ (V)	E_{S1-S0} (eV)	HOMO (eV)	LUMO (eV)	$\Delta E_{HOMO-LUMO}$
2MP (MeCN)	1.18	−2.41	3.59	2.94	−7.96	−0.391	7.57
7P (MeCN)	1.24	−2.32	3.56	2.93	−8.02	−0.769	7.25
4OP (MeCN)	1.26	−2.29	3.55	2.89	−8.04	−0.773	7.27
10P (1:1 MeCN/PhH)	1.30 ($E_{1/2}$ = 1.27)	−2.29	3.59 (3.56)	3.13 (MeCN)	−7.98	−0.867	7.11
pyrene (1:1 MeCN/PhH)	1.28	−2.16	3.51	3.16 (MeCN)	−7.96	−1.04	6.92

led to the rapid formation of byproducts, as shown in Figure 3b. The radical anion of 7P displayed greater stability, indicated by the smaller byproduct oxidation peaks observed around −0.4 and −1.3 V vs SCE. Pyrene, the planar parent compound, showed the highest stability upon reduction indicated by the lack of any reoxidation waves corresponding to the oxidations of byproducts generated from fast following chemical reactions (Figure 3e). Unlike the reductions, the oxidations showed no reversibility even at scan rates beyond 50 V/s for all the compounds in this study, except 10P. In addition, upon continuous potential cycling over the range that encompassed the first oxidation and first reduction waves, the loss of reversibility in the reduction wave became more pronounced with the increasing number of potential scans. The products of this reaction formed an insoluble film on the surface of the platinum-working electrode, which altered the electrochemical behavior of these compounds as well as that of the internal potential standard, ferrocene. Such electrochemical behavior could pose problems in ECL upon radical ion annihilation.

10P, the pyrenophane with the longest aliphatic bridge between the 2 and 7 positions, displayed slightly different electrochemistry. Upon scanning in the positive direction, a quasi-reversible oxidation was observed at peak potential of 1.30 V vs SCE. At scan rate beyond 1 V/s, peak current ratio (i_{pa}/i_{pc}) unity was obtained. The stability of the radical cation was indicated by the absence of the characteristic reduction waves of chemical byproducts observed at around 0.3 and 0 V vs SCE. Similar to other compounds in this study, a reversible one electron reduction was observed at half-wave potential of −2.29 V vs SCE. There was also a smaller reduction wave observed at around −2.2 V vs SCE. This smaller wave can probably be attributed to a hard to remove impurity. Reoxidation of this impurity as well as other byproducts from the fast following chemical reactions were observed at potentials around −1.9, −1.2, and −0.8 V vs SCE, as shown in Figure 3d. Upon potential cycling, an insoluble film was formed despite the enhanced stability of the radical cation. This film formation process, however, occurred at a much slower rate when compared to other compounds in this study. This again could pose problems in obtaining stable ECL via radical annihilation.

A previous study from Bodwell et al. showed an increase in the potential for oxidation with increasing bending within the molecule.[14] Our electrochemical data showed a similar trend, with 2MP displaying the least positive oxidation, followed by 7P, 4OP, pyrene, and 10P. However, it is not possible to directly interpret this trend to the degree of bending due to the irreversibility of the oxidation wave observed in these compounds. Like any irreversible cyclic voltammetric peak, the oxidation peak potentials of these compounds shift with scan rate and concentration, as well as the kinetics of the following chemical reactions so that peak potentials obtained from voltammetry could not be viewed as the thermodynamic potentials for oxidation, but as a reference to the thermodynamic oxidation potentials. Unlike the oxidations, the reductions in all the compounds showed nernstian behavior and among the five compounds studied 2MP showed the most negative reduction potential, whereas pyrene showed the least negative potential. This trend suggests a possible link between molecular geometry and the reduction potential in which the most planar compound shows the least negative reduction potential. 10P, though substantially more planar than 4OP, showed the same reduction potential. This could be explained by the difference in the peak shape between 4OP and 10P. The presence of an overlapping reduction peak from the impurity created a slight difficulty in obtaining an accurate measurement of the standard reduction potential of the compound itself.

We were also interested in using semiempirical calculations to locate the molecular orbitals of the compounds in this study and to validate the shift in redox potentials with increasing nonplanarity within the molecule. From the AM1 calculations that we performed to determine the optimized ground state geometry of the five compounds, the calculated energy levels of the HOMO and LUMO of each compound were compared to the energy levels determined by voltammetric data. These values are given in Table 2. Upon comparing the peak potential for the oxidation and half-wave potential for the reduction to

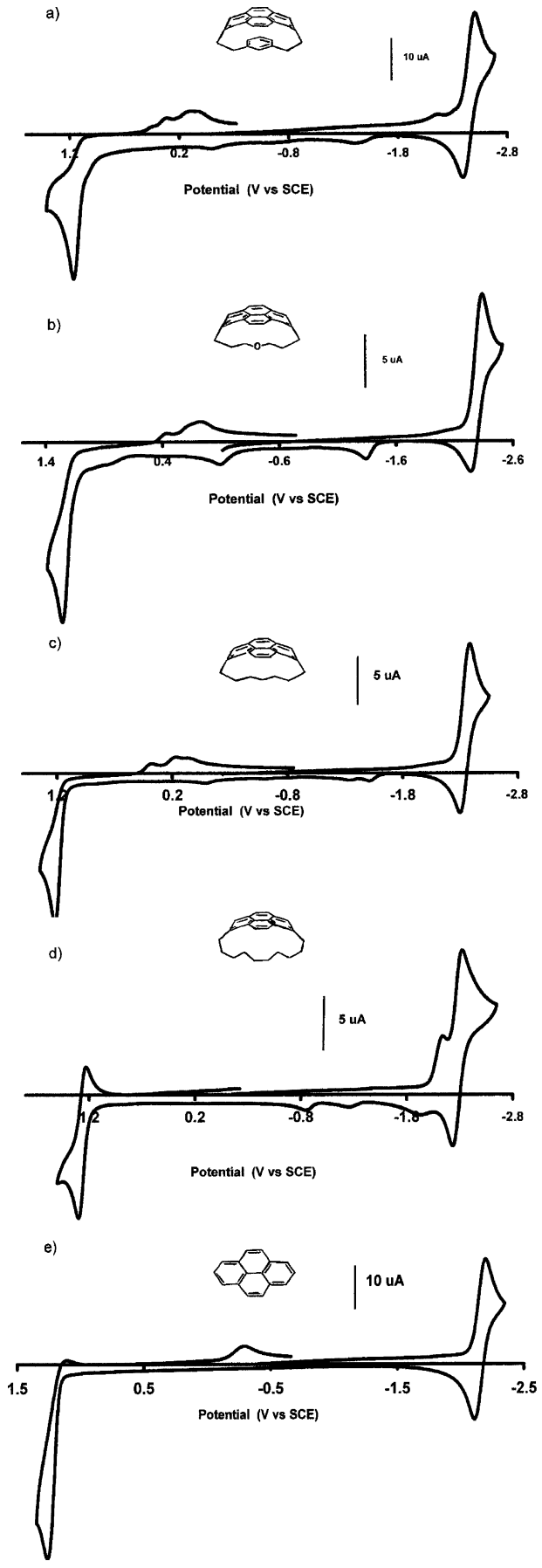

Figure 3. Cyclic voltammograms of 1 mM solution of (a) 2MP, (b) 4OP, and (c) 7P in 0.1 M $TBAPF_6$ in MeCN at a platinum electrode. Voltammograms of 10P and pyrene in 0.1 M $TBAPF_6$ in 1:1 MeCN/PhH are shown in (d) and (e), respectively. Scan rate: 200 mV/s.

the calculated energy level of the HOMO and LUMO, there appears to be a correlation between the reduction potentials and the LUMO energies. The results showed that the LUMO energy increases with increasing bending in the molecule, whereas the HOMO energy remains essentially constant for all the compounds in this study. The increase in the LUMO energy correlates with the increase in the reduction potential, as shown in the electrochemistry. However, without the standard potential of oxidation for each of the compounds, we could not validate the trend observed in the HOMO energies. The increase in the HOMO energy contributes to an increase in the overall HOMO−LUMO energy gap for the severely bent compounds. Pyrene, the only planar compound in this study, displayed the smallest energy gap, which mirrors the annihilation energy obtained in the electrochemistry. 4OP and 7P showed very similar HOMO−LUMO energy gaps as well as annihilation energy, suggesting similarities in their geometry in terms of the degree of bending.

On the basis of the HOMO−LUMO energy gap for these compounds, one could expect the lowest absorption energy of the bent molecules to be blue-shifted with respect to the planar compound, pyrene. However, as shown in Figure 2a, the lowest absorption energy (the last *p* band) for all four pyrenophanes was red-shifted by about 5 nm when compared to pyrene. The observed red shift does not agree well with the electrochemical annihilation energy, which disagrees with the theoretical HOMO−LUMO energy gap. This could be attributed to the difference between the oxidation peak potential and the thermodynamic potential of oxidation of the compound. Thus, depending on the kinetics of the following chemical reactions, the oxidation peak potential could appear to be more or less positive than the true thermodynamic potential, which could have contributed to the over- or underestimation of the annihilation energy.

Overall, the reduction potentials agree well with the semiempirical calculations in which 2MP appears to be the most nonplanar, followed by 7P, 4OP, 10P, and pyrene. This trend, however, does not support previous results obtained by Bodwell et al. The degree of nonplanarity was previously determined from the bending angle θ, calculated at the AM1 level of theory.[17] These results suggested that 4OP (108.3°) is the most nonplanar, followed by 2MP (106.6°), 7P (104.6°), and 10P (54.4°). This is due to the presence of the oxygen atom, which effectively shortened the bridge across the 2 and 7 positions because C−O bonds are generally slightly shorter than C−C bonds.[4] A shorter bridge, thus, induces a more bent conformation for 4OP when compared to 7P and 2MP. However, due to the similarities between 2MP, 7P, and 4OP, it is difficult to accurately determine the true conformation of each of the molecules and that minor differences in the calculations could lead to a slightly different conformation as well as energy levels. More computations are required and are currently under investigation.

As a final note, the total free energy of the annihilation reaction, $\Delta H_{ann} = \Delta G_{ann} + T\Delta S$, is based on the difference between the peak potential of the oxidation and the half-wave potential of the reduction wave in the cyclic voltammogram with correction for entropy effects (~0.1 eV). This energy, which becomes available upon radical ion annihilation, should be greater than the singlet energy (E_s), as determined from the fluorescence spectrum to directly populate the singlet-excited state. As calculated from the fluorescence spectra, all compounds in this study are energy-sufficient for the singlet-excited states to be directly populated upon radical ion annihilation. This conclusion is valid, even though the oxidation half-reaction is

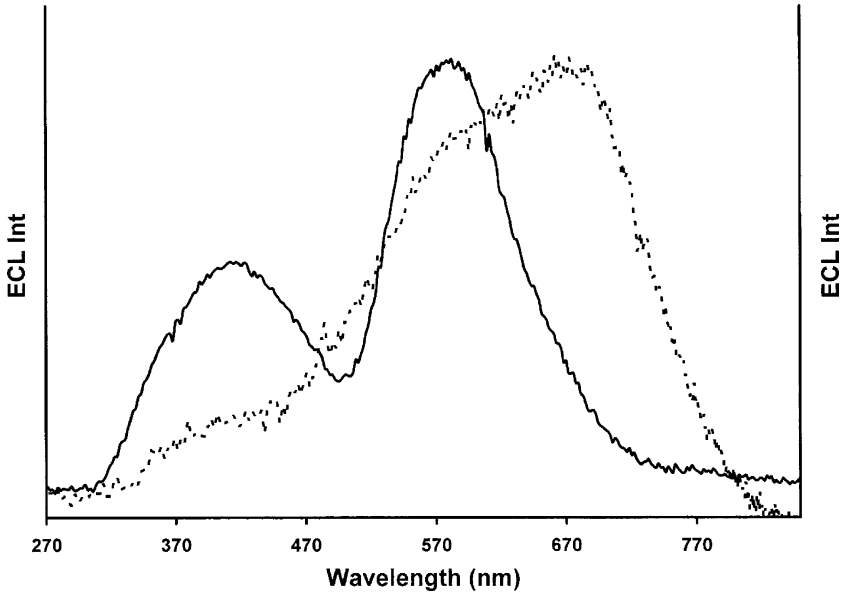

Figure 4. ECL spectra of 1 mM of 10P and 10 mM of BPO in 0.1 M $TBAPF_6$ in MeCN/PhH with pulsing between 0 and −2.3 V (vs SCE) (solid line) and 1 mM 10P in 0.1 M $TBAPF_6$ in the same solvent with pulsing (0.1 s) between 1.31 and −2.3 V (vs SCE) (dotted line).

irreversible, because a following chemical reaction would shift the measured potential to less positive values. Because E_s is generally higher than the triplet energy (E_t), the triplet-excited state could also be generated in the same process. Thus, the observed ECL emission from these compounds would be a result of direct singlet emission as well as emission from triplet−triplet annihilation (TTA). However, due to the instability of the radical cations, BPO, a coreactant capable of generating a bulk oxidant in the negative potential region, was introduced to the systems as discussed in the next section.

Electrogenerated Chemiluminescence (ECL). The ECL results are summarized in Table 1. To generate ECL by the annihilation route, the platinum working electrode was pulsed between the peak potentials where oxidized and reduced forms were alternately produced. The ECL mechanism leading to both monomer and excimer emission via radical ion annihilation can be represented as

Mechanism I

$$Py + e \rightarrow Py^{\bullet -} \quad (10)$$

$$Py - e \rightarrow Py^{\bullet +} \quad (11)$$

$$Py^{\bullet +} + Py^{\bullet -} \rightarrow {}^1Py^* + Py \text{ or } Py_2^* \quad (12)$$

$$Py^{\bullet +} + Py^{\bullet -} \rightarrow {}^3Py^* + Py \quad (13)$$

$${}^3Py^* + {}^3Py^* \rightarrow {}^1Py^* + Py \text{ or } Py_2^* \quad (14)$$

$${}^1Py^* \rightarrow Py + h\nu_1 \text{ (monomer)} \quad (15)$$

$$1Py_2^* \rightarrow 2Py + h\nu_2 \text{ (excimer)} \quad (16)$$

Among the five compounds, very weak ECL was observed from 10P and pyrene upon radical ion annihilation (Figures 4 and 5). As shown in the spectra, extra long wavelength components were observed at around 650 and 680 nm for pyrene and 10P, respectively. These emission peaks were red shifted from the emission wavelengths of both the monomer and excimer and most likely represent emission from byproducts upon annihilation, owing to the instability of the cation.[2,18] Under the same experimental conditions, no measurable emission was observed from 2MP, 4OP, and 7P, probably because of the enhanced instability of the cations as well as the anions in solution. In all cases, film formation on the surface of the electrode was evident after pulsing for 2 min, similar to what was observed upon extensive potential cycling in the same region.

To circumvent this problem of radical cation instability, a known ECL coreactant, BPO, was used to generate a bulk oxidant to participate in the homogeneous electron-transfer reaction with the electrogenerated radical anion.[9,19,20] The proposed ECL mechanism leading to both monomer and excimer emission in the presence of BPO can be represented as

Mechanism II

$$Py + e \rightarrow Py^{\bullet -} \quad (17)$$

$$BPO + e \rightarrow BPO^- \quad (18)$$

$$BPO + Py^- \rightarrow BPO^- \quad (19)$$

$$BPO^- \rightarrow Ph{-}CO_2^- + Ph{-}CO_2^{\bullet} \quad (20)$$

$$Ph{-}CO_2^{\bullet} + Py^{\bullet -} \rightarrow {}^1Py^* + Ph{-}CO_2^- \quad (21)$$

$$Ph{-}CO_2^{\bullet} + Py^{\bullet -} \rightarrow {}^3Py^* + Ph{-}CO_2^- \quad (22)$$

$$Ph{-}CO_2^{\bullet} + {}^3Py^* \rightarrow Py^{\bullet +} + Ph{-}CO_2^- \quad (23)$$

$$PH{-}CO_2^{\bullet} + Py \rightarrow Py^{\bullet +} + Ph{-}CO_2^- \quad (24)$$

$$BPO + {}^3Py^* \rightarrow Py^{\bullet +} + BPO^- \quad (25)$$

Followed by reactions 12−16.[9,19,20]

When an electrode was immersed in a solution of 10P containing 10 mM of BPO and was pulsed between 0 V and the reduction peak potential, a bright blue light that was visible by eye in a darkened room was produced at the electrode surface. The ECL spectrum of 10P obtained in MeCN/PhH (1:1) containing 0.1 M of $TBAPF_6$ as supporting electrolyte is shown in Figure 4. Although the light appeared to be fairly

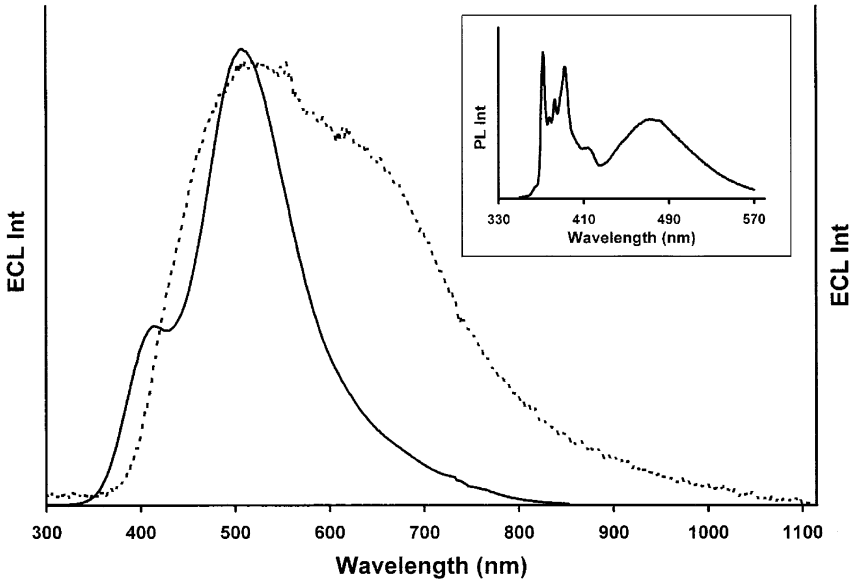

Figure 5. ECL spectra of 1 mM of pyrene and 10 mM of BPO in 0.1 M $TBAPF_6$ in MeCN with pulsing between 0 and −2.2 V (vs SCE) (solid line) and 1 mM pyrene in 0.1 M $TBAPF_6$ in the same solvent with pulsing (0.1 s) between 1.28 V and −2.16 V (vs SCE) (dotted line). Inset: Fluorescence spectrum of 1 mM of pyrene in MeCN. Excitation wavelength: 335 nm.

strong during the first few minutes, the instability of the radical cations as well as the side reactions from the reduction of BPO presented problems in obtaining stable ECL over a period of time. As shown in the spectrum, there are two defined emission peaks around 420 and 589 nm. On the basis of previous studies of pyrene and pyrene derivatives, these two peaks probably correspond to the monomer and excimer emission of 10P.[2,18] However, the byproducts generated upon BPO reduction and the quasi-reversible oxidation of the compound itself could also contribute to the longer wavelength emission observed in the spectrum.[21] When compared to the fluorescence spectrum (Figure 2b), the monomer emission of 10P in the ECL spectrum appears to be broader in shape, structureless, and slightly shifted to lower energy (∼15 nm). This is probably due to an inner filter effect as a result of the high concentrations of the compound needed to obtain measurable ECL, as well as the difference in resolution between the two instruments where the spectra were collected. In addition, the monomer and the "excimer-like" emission peak of 10P are better-resolved when compared to the ECL spectrum of pyrene obtained under the same conditions (Figure 5). Such behavior was observed in all the other compounds in this study, as shown in Figure 6. Among the five compounds studied, 10P showed the most stable ECL, probably because of the enhanced stability of the radical cation, as observed in its electrochemistry. However, the ECL obtained from 10P appeared to be the least intense, even in the first cycle when film formation had not yet occurred. This may be attributed to the difference in the experimental conditions to accommodate solubility. Among the compounds studied, 4OP showed the lowest ECL stability, as indicated by the loss of ECL after 6 min of pulsing between the redox peak potentials in addition to film formation that was evident upon radical ion annihilation.

If the long wavelength emission can be ascribed to the excimer, the integrated area ratio between the monomer and excimer should be a function of the geometry of the compound, in which planar compounds would favor excimer formation. As shown in Figures 4 and 5, the monomer/excimer ratio of 10P is slightly higher than that for pyrene, suggesting that 10P is slightly more bent than pyrene. However, 2MP showed the highest monomer/excimer ratio, even when compared to pyrene, the only planar compound in this study. In addition, the monomer/excimer ratio of these compounds appeared to change with time; therefore the spectra shown in Figure 6 were each obtained with a cleaned and polished electrode. As expected, these results do not agree well with the trend observed in the electrochemistry mainly because the formation of excimer in the presence of BPO is related to the geometry of the compound as well as the stability of the radical cation, which differs for each compound. As observed in Figure 5, more excimer emission of pyrene was evident in the ECL spectrum when compared to the fluorescence spectrum obtained at the same concentration. The fact that the excimer emission is much more intensive in the ECL spectra than in the fluorescence spectra of the same concentration may be due to the different modes of excimer formation. In fluorescence spectroscopy, the excited molecule requires an encounter with an unexcited molecule to generate an excimer. In ECL, excimers could be formed directly in the electron-transfer reaction between radical cations and anions or by TTA. Previous research by Akins et al. suggests that radical cations could be generated via oxidation of the triplet by the intermediate radical of BPO or by BPO itself (eqs 23 and 25); these cations could then participate in radical ion annihilation, thus forming a larger amount of excimers.[9,19] Chandross and co-workers, however, assumed that the potential for oxidation of the benzoate ion (i.e., $Ph-CO_2^- \rightarrow Ph-CO_2^\bullet + e$) was around 1.5 V vs SCE rather than 0.8 V vs SCE as proposed in Akins' work.[20] In this case, radical cations could be generated via direct oxidation of the ground-state molecule by the intermediate benzoate radical, as shown in eq 24. Because no further research was conducted to validate either of the values, both values were considered in our proposed ECL mechanisms. However, if Chandross' suggested value were closer to the true oxidation potential of the benzoate ion, direct population of the singlet excited state would be possible (eq 21). This will lower the yield of the triplet states available for TTA and less excimer emission will be observed. But in either case, radical cations could be generated either via reactions shown in eqs 23 and 25, as suggested by Akins et al., or via eq 24 based on Chandross' theory. The difference in the monomer/excimer ratio between similar compounds such as 2MP and 7P could also be explained by the difference in the stability of the

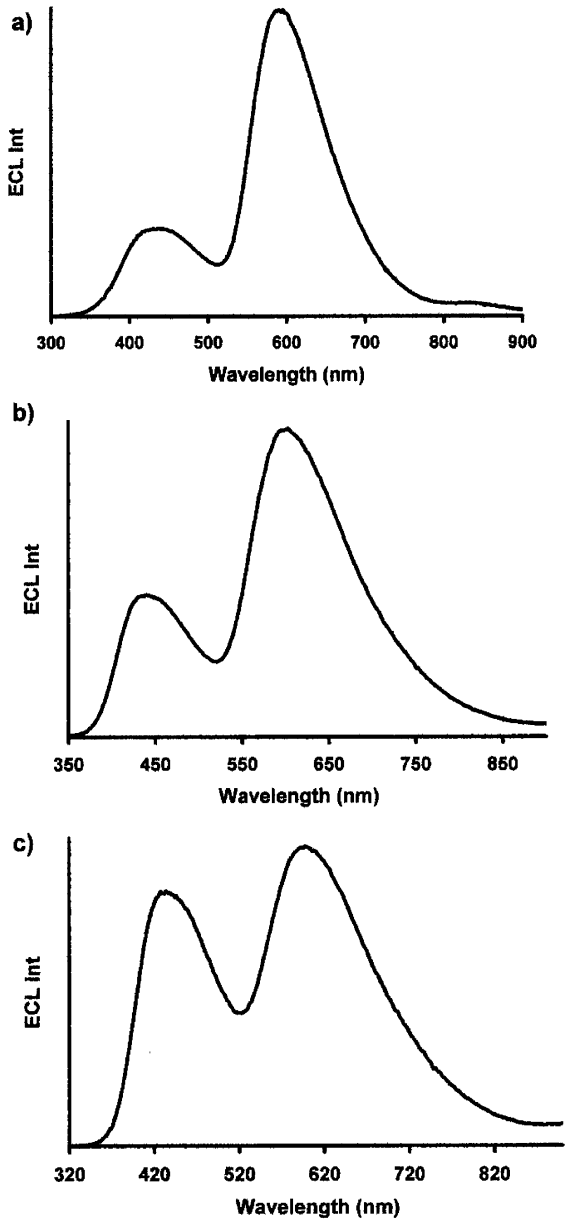

Figure 6. ECL spectra of 1 mM of (a) 2MP, (b) 4OP, and (c) 7P in the presence of 10 mM BPO in 0.1 M $TBAPF_6$ in MeCN with pulsing (0.1 s) between 0 V and their respective reduction peak potential.

cations. A relatively more stable cation has a longer lifetime and therefore a better chance to undergo electron transfer with an anion to form an excimer.

Conclusion

The photophysical, electrochemical, and ECL properties of pyrene and four novel pyrenophanes were investigated. Overall, pyrenophanes with a shorter bridge across the 2 and 7 positions showed less-positive peak potentials for oxidation and more negative reduction potentials. This result agrees with the AM1 semiempirical calculations in which the LUMO energy increases with decreasing planarity within the molecule. However, the HOMO energy remains essentially constant for all the compounds in this study. The nonplanarity in these compounds effectively lowered the fluorescence quantum yield in addition to red-shifting both the absorption and emission wavelengths when compared to pyrene, the planar molecule. The instability of the cation as well as the anion in some systems gave rise to a lack of ECL or low ECL intensity upon radical ion annihilation. In the presence of BPO, more intense ECL was obtained. The ECL spectra, however, showed monomer emission in addition to broad "excimer-like" emission that was not present in fluorescence spectroscopy.

Acknowledgment. This work was supported by the Robert A. Welch Foundation, the Texas Advanced Research Program (0103), IGEN Inc., and the Natural Sciences and Engineering Research Council (NSERC) of Canada.

References and Notes

(1) For reviews on ECL see: (a) Knight, A. W.; Greenway, G. M. *Analyst* **1994**, *119*, 879. (b) Faulkner, L. R.; Bard, A. J. *Electroanalytical Chemistry*; Marcel Dekker: New York, 1977; Vol. 10, p 1. (c) Bard, A. J.; Debad, J. D.; Leland, J. K.; Sigal, G. B.; Wilbur, J. L.; Wohlstadter, J. N. In *Encyclopedia of Analytical Chemistry: Applications, Theory and Instrumentation*; Meyers, R. A., Ed.; John Wiley & Sons: New York, 2000; Vol. 11, p 9842 (see also references therein).

(2) Fleet, B.; Kirkbright, G. F.; Pickford, C. *J. Electroanal. Chem.* **1971**, *30*, 115.

(3) (a) Chandross, E. A.; Longworth, J. W.; Visco, R. E. *J. Am. Chem. Soc.* **1965**, *87*, 3259. (b) Maloy, J. T.; Bard, A. J. *J. Am. Chem. Soc.* **1971**, *93*, 5968.

(4) Bodwell, G. J.; Fleming, J. J.; Miller, D. O. *Tetrahedron* **2001**, *57*, 3577.

(5) (a) Bodwell, G. J.; Fleming, J. J.; Mannion, M. R.; Miller, D. O. *J. Org. Chem.* **2000**, *65*, 5360. (b) Bodwell, G. J.; Bridson, J. N.; Houghton, T. J.; Kennedy, J. W. J.; Mannion, M. R. *Chem. Eur. J.* **1999**, *5*, 1823. (c) Bodwell, G. J.; Merner, B. L. Unpublished results.

(6) Grabner, E. W.; Brauer, E. *Ber. Bunsen-Ges. Phys. Chem.* **1972**, *76*, 111.

(7) Hercules, D. M.; Chang, J.; Werner, T. C. *J. Am. Chem. Soc.* **1970**, *92*, 5560.

(8) Zu, Y.; Bard, A. J. *Anal. Chem.* **2000**, *72*, 3223.

(9) Cruz, T. D.; Akins, D. L.; Birke, R. L. *J. Am. Chem. Soc.* **1976**, *98*, 1677.

(10) White, H. S.; Bard, A. J. *J. Am. Chem. Soc.* **1982**, *104*, 6891.

(11) Windsor, M. W.; Dawson, W. R. *J. Phys. Chem.* **1968**, *72*, 3251.

(12) Masui, M.; Sayo, H.; Tsuda, Y. *J. Chem. Soc. B* **1968**, 973.

(13) McCord, P.; Bard, A. J. *J. Electroanal. Chem.* **1991**, *318*, 91.

(14) Bodwell, G. J.; Bridson, J. N.; Cyranski, M. K.; Kennedy, J. W.; Krygowski, T. M.; Mannion, M. R.; Miller, D. O. *J. Org. Chem.* **2003**, *68*, 2089.

(15) Mehlhorn, A.; Schwenzer, B.; Schwetlick, K. *Tetrahedron* **1977**, *33*, 1489.

(16) (a) Martinho, J. M. G.; Sousa, A. T. R.; Torres, M. E. O.; Fedorov, A. *Chem. Phys.* **2001**, *264*, 111. (b) Castanheira, E. M. S.; Martinho, J. M. G. *Chem. Phys. Lett.* **1991**, *185*, 319.

(17) AM1 Semiempirical calculations performed with HyperChem by Hypercube, Inc., Gainesville, FL.

(18) Birks, J. B.; Christopherou, L. G. *Spectrochim. Acta* **1963**, *19*, 401.

(19) Akins, D. L.; Birke, R. L. *Chem. Phys. Lett.* **1974**, *29*, 428.

(20) Chandross, E. A.; Sonntag, F. I. *J. Am. Chem. Soc.* **1966**, *88*, 1089.

(21) (a) Urano, T.; Kitamura, A.; Sakuragi, H.; Tokumaru, K. *J Photochem.* **1984**, *26*, 69. (b) Urano, T.; Sakuragi, H.; Tokumaru, K. *Chem. Lett.* **1985**, 735.